

Simulation of Ultrasound Produced by Concentric Ring Transducer Phased Array to Treat Urinary Bladder Using Waveform Diversity Method

Ashraf Talaat Ibrahim, Nour Hassan Ismail

EEE Department, Faculty of Engineering, Alexandria University, Alexandria, Egypt

Email address

ashraftalaat@yahoo.com (A. T. Ibrahim), nhassan58@live.com (N. H. Ismail)

Citation

Ashraf Talaat Ibrahim, Nour Hassan Ismail. Simulation of Ultrasound Produced by Concentric Ring Transducer Phased Array to Treat Urinary Bladder Using Waveform Diversity Method. *American Journal of Biomedical Science and Engineering*. Vol. 4, No. 1, 2018, pp. 7-12.

Received: March 4, 2017; **Accepted:** January 29, 2018; **Published:** February 12, 2018

Abstract: The waveform diversity method is applied for the simulation of focused ultrasound produced by concentric ring transducer phased arrays which are put in front of a tumor of human Urinary bladder. The waveform diversity method computes the output pressure in a certain volume. The pressure deposition due to the array used is converted to therapeutic temperature for tumor treatment. Simulation and results show that the concentric ring transducer phased arrays producing pressure determined by waveform Diversity Method can be applied successfully for urinary bladder tumor treatments.

Keywords: Ultrasound, Phased Array, Urinary Bladder, Waveform

1. Introduction

Pressure generated by ultrasound phased arrays are calculated by superposing the pressure produced by individual transducer sources. There are many methods to get pressure inside biological media such as Rayleigh–Sommerfield integral, the rectangular radiator method, and the spatial impulse response method. The analytical approaches for those methods are slow due to the large number of calculations [1]. The waveform diversity method determines the excitation signals applied to the phased array elements and produces a beam pattern that closely matches the desired power distribution [2]. The optimization algorithm solves the covariance matrix of the excitation signals through semidefinite programming subject to a series of quadratic cost functions and constraints on the control points. Section II discuss the software used for analytical approach depending on the waveform diversity method. Section III explain the model under investigation and how the phased array is used. Section IV contain the pressure and temperature distributions while section V present conclusions.

2. Analytical Approach

The soft ware used for the pressure calculation is performed on a 2.4 GHz

Pentium 4 PC (1 G byte random access memory) running the Windows XP operating system. All routines are written in the C language, compiled by Microsoft VISUAL C/C – Version 7.0, and called by MATLAB 7.1 as MEX files.

Now let's walk through writing a script that uses the waveform diversity method to calculate the pressure field generated by a concentric ring transducer phased arrays under continuous wave excitation.

1-General parameters of array in meters.

a) The number of rings in the array. b) The width of all rings in meters. c) The edge-to-edge spacing of the rings in meters.

2- set up our coordinate grid.

Now we need to enter the arguments that will be used

a) The min and max arguments sets the boundaries of the calculation grid. b) The delta argument is the distance from each point to its nearest neighbor and most is in the form of a matrix.

3- Define the three layers lung media and its parameters.

The layers are a) bolus b) skin. c) muscle. d) tumor.

4- Finally we calculate the pressure field using the transducer and coordinate

For a continuous-wave excitation, the pressure generated by a phased array at a spatial coordinate r and at time t is defined by [3].

$$p(r, t) = \sum_{m=1}^M p_m(r) w_m(t) \quad (1)$$

Where M is the number of array elements, $p_m(r)$ is the complex pressure produced by the m th array element at r when excited by a sinusoidal signal with unit amplitude and zero phase, and $w_m(t)$ is a sinusoidal input multiplied by a complex weight that contains the phase and amplitude applied to the m th array. A sequence of several beam patterns, equation (1) becomes

$$p(r, n) = \sum_{m=1}^M p_m(r) w_m(n) = \bar{p}(\bar{r}) w(\bar{n}), n=1, 2, \dots, N \quad (2)$$

where $\bar{p}(\bar{r})$ is a $1 \times M$ row vector that is populated with the values $p_m(r)$ and $\bar{w}(\bar{n})$ is an $M \times 1$ column vector, which represents the excitation applied to the array for an individual beam pattern indexed by n . Thus, $p(r, n)$ describes a sequence of N different beam patterns, and the ultrasound phased array repeatedly cycles through these multiple focus patterns during the hyperthermia treatment. The power depositions from the individual beam patterns are computed with the plane-wave approximation and then superposed, giving

$$Q(r) = \frac{\alpha}{\rho c} \sum_{n=1}^N p(r, n) p^*(r, n) \quad (3)$$

where $Q(r)$ is the total power deposition, α is the absorption coefficient, ρ and c represent the density of the medium and the speed of sound, respectively, and the superscript $*$ represents the conjugate transpose. Substituting equation (2) into equation (3), the expression for the power deposition becomes

$$\begin{aligned} Q(r) &= \frac{\alpha}{\rho c} \sum_{n=1}^N \bar{p}(\bar{r}) w(\bar{n}) \bar{w}^*(\bar{n}) p^*(r) \\ &= \frac{\alpha}{\rho c} \bar{p}(\bar{r}) \bar{R}_p^*(r) \end{aligned} \quad (4)$$

where R is an $M \times M$ Hermitian matrix that is equivalent to the covariance matrix defined in [4]. The deterministic beam synthesis problem is directly solved by sequentially assigning each column of $R^{1/2}$ to a complex array excitation $\bar{w}(n)$, where $R^{1/2}$ is the Hermitian square root of R . The matrix R is rank deficient, so the number of distinct excitation signals is significantly reduced through singular value decomposition. Here, the rank of the matrix R defines the number of discrete excitations N , and the singular value decomposition is defined as $R = USV^*$, where U and V are $M \times N$ matrices with orthonormal columns, and S is a diagonal $N \times N$ matrix that contains the singular values of R . The reduced solution is then represented by

$$X = US^{1/2} \quad (5)$$

where $S^{1/2}$ is the matrix square root of S , and each column of the $M \times N$ matrix X contains a distinct array excitation $w(n)$.

Thus, the number of unique array excitations required to achieve the optimal covariance matrix R is reduced from M , the number of array elements, to a much smaller number given by $N = \text{rank}(R)$.

One objective function that is commonly deployed in hyperthermia applications attempts to deliver relatively uniform power within the tumor region when minimizing the power deposition in normal tissue. The optimization problem solved here is as follows:

$$\bar{p}(\bar{r}_0) \bar{R}_p^*(r_0) - \bar{p}(\mu) \bar{R}_p^*(\mu) > 0, \mu \in \Omega_N$$

$$\bar{p}(v) \bar{R}_p^*(v) \geq 0.9 \bar{p}(\bar{r}_0) \bar{R}_p^*(r_0), v \in \Omega_T$$

$$\bar{p}(v) \bar{R}_p^*(v) \leq 1.1 \bar{p}(\bar{r}_0) \bar{R}_p^*(r_0), v \in \Omega_T$$

$$R \geq 0$$

$$\sum R_{mm} = \gamma \quad (6)$$

where μ denotes one of the N_N control points in the normal tissue region Ω_N , v denotes one of the N_T control points in the tumor region Ω_T , and r_0 is a characteristic point within Ω_T , i.e., r_0 is a representative point in the tumor. The cost function maximizes the difference between the power at r_0 and the power at all normal tissue control points μ , given that this difference is nonnegative. The first constraint (combined with the restriction >0) guarantees that the power at r_0 is always larger than the power at μ . The second and the third constraints ensure that the power deposited at the tumor control points v is not more than 1.1 times and not less than 0.9 times the power at r_0 . The fourth constraint defines the matrix R as a positive semi-definite Hermitian matrix. The fifth constraint indicates that the total input power is specified by the constant γ [5]. The first four constraints are the same as in [4], and the fifth constraint in equation (6) specifies the total input power instead of an average uniform power. The function

$p(r) = \bar{p}(\bar{r}) \bar{R}_p^*(r)$ is convex; therefore, the optimization problem in (6) can be solved with public domain software for convex optimization, [6], [7].

An ultrasound phased array generates a focus by adjusting the phases of the excitation signals. For continuous-wave excitations, a single focus is produced by phase conjugation [8], where the negative of the phase of the complex pressure transfer function evaluated at the focus for each array element defines the phase of the excitation signal for that element. With this approach, the phased array generates constructive interference at each focal spot.

The pressures $p_m(r)$ generated by the individual array elements at individual control points are computed with the fast near-field method [9]. The pressure field in a 3-D volume for an array excitation $\bar{w}(n)$ is calculated with the angular spectrum approach combined with the fast near-field method [10]. The fast near-field method calculates the pressure generated by the phased array in an input plane, and the angular spectrum approach propagates the pressure in the 3-D volume. Each steady-state power deposition is computed according to equation (3), and the contributions from N scans

are then superposed. The temperature is simulated with the steady-state bioheat transfer equation (BHTE):

$$k\nabla^2 T(r) - W_b C_b T(r) + Q(r) = 0 \quad (7)$$

where K is the thermal conductivity of tissue, C_b is the specific heat of blood, W_b is the blood perfusion rate, and T is the tissue temperature increase relative to the baseline arterial blood temperature (37°C). Equation (7) is solved with an iterative finite-difference scheme. [10]

3. Modeling Under Investigation

This section describe briefly the 10 elements rings array shown in figure 1 (high = 2mm, width = 0.5mm, space between elements = 0.00075m, $f = 1\text{MHz}$, the outer ring diameter = 1.175 cm). The urinary bladder model shown in figure 2 and the phased array in x-y plane is located parallel to the human body front of urinary bladder tumor.

4. Pressure and Temperature Distributions

The numerical analysis using the waveform diversity method for 10 rings element 2D planar phased is depicted in this section. The width of all rings = $0.5\text{e-}3\text{ m}$ with a $7.5 \times 10^{-4}\text{ m}$ ($\lambda/2$) space between adjacent elements in both x and y directions. The array is located in the x-y plane at $z=0\text{ cm}$ and centered at the origin of the coordinate system. The z axis is coincident with the normal evaluated at the center of the array.

The excitation frequency is 1 MHz, the speed of sound is 1500 m/s, and the attenuation coefficients $\alpha = 1\text{dB/cm/MHz}$.

The total extent of the array aperture is 1.75 cm radius. This array is put in front of the Urinary bladder. The initial evaluations of the pressure field generated by this 10 rings element phased array in x-y and x-z planes in the Urinary bladder volume directions are shown in figure 3.

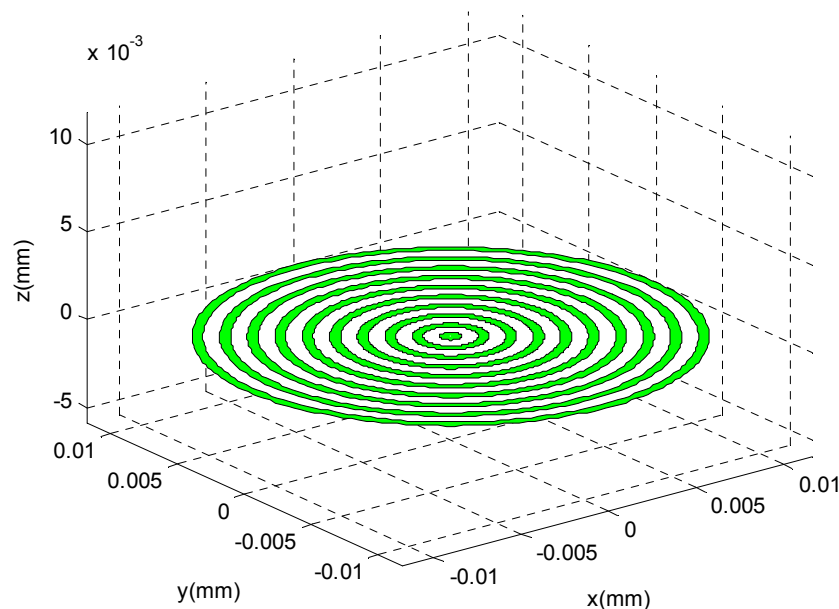


Figure 1. The structure of the ringphased array.

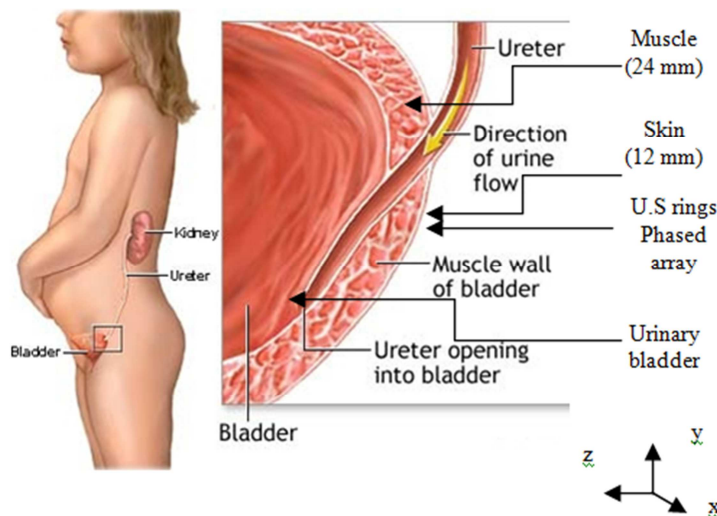


Figure 2. Urinary bladder and the phased array.

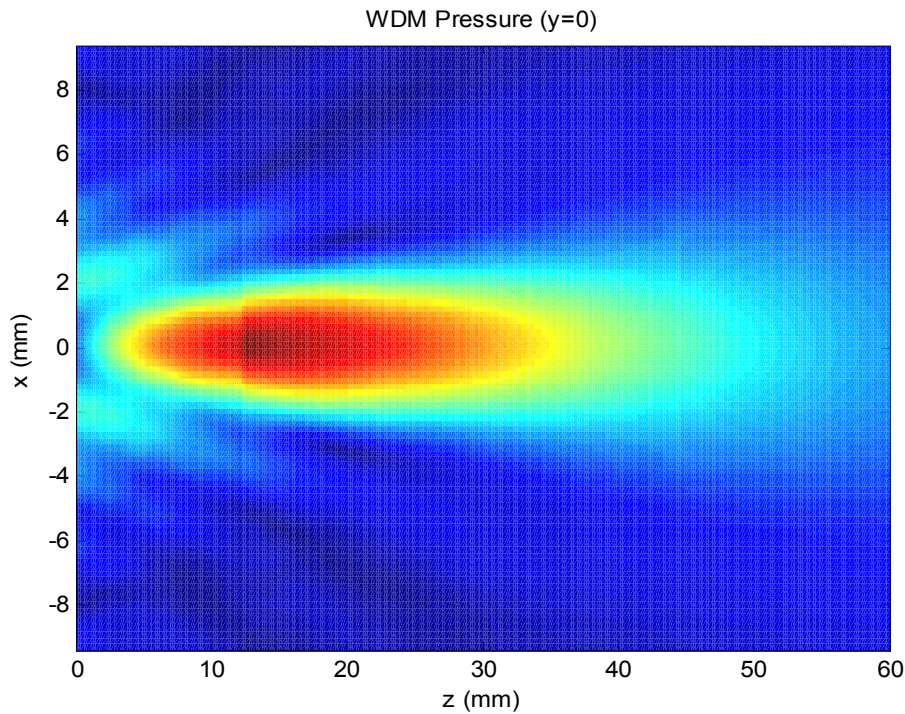
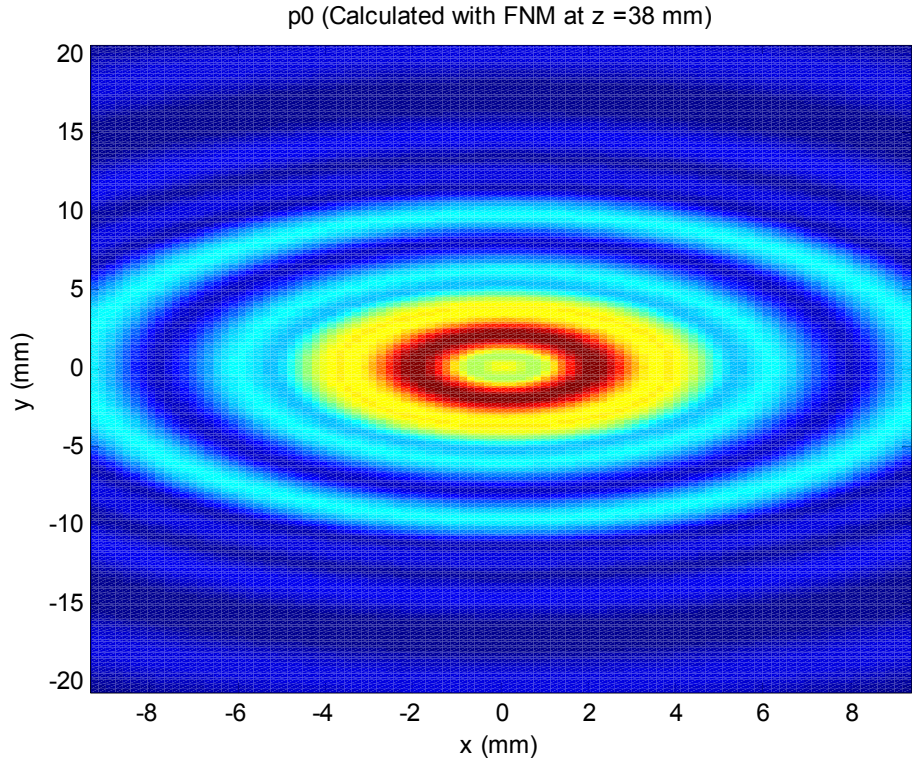


Figure 3. The ultrasound pressure at $z=38$ mm.

With a sampling interval of 7.5×10^{-4} m ($\lambda/2$), the computational volume is discretized to a $273 \times 273 \times 161$ point grid. Figure 4 shows the temperature generated by this 10 rings element phased array in the $y=0$ plane. The array elements are phased such that a single focus is produced at

(0,0,38) mm.

Symmetric multiple focusing is realized with mode scanning [14]. Mode scanning utilizes the symmetry of the phased array to generate a symmetric focal pattern while canceling the pressure along one or more planes of symmetry.

A symmetric phased array is typically divided by these symmetric planes in to two or four equal sections. The array elements in each section are indexed according to the planes of symmetry such that the distances from each pair of elements to any point on the plane of symmetry are equal. The computational volume is also divided into an equal number of sections by these same planes of symmetry. The rotational signals are defined such that the phases applied to elements on opposite sides of each plane of symmetry are

offset by π , which causes pressure cancellations along the planes of symmetry. A symmetric, focused power distribution is formed by applying rotational excitation signals to each symmetric group of elements and then calculating the phase of each group with phase conjugation or waveform diversity.

The same array can be used for producing multi focus in the same tumor volume at 38mm and the temperature distribution is shown in figure 5.

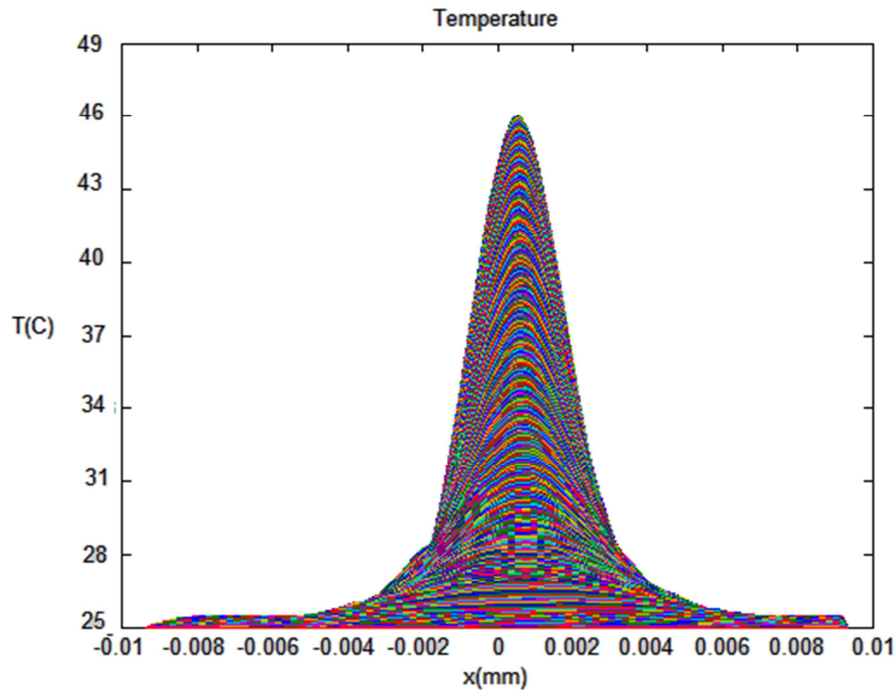


Figure 4. The temperature distribution in the treatment volume at (0,0,38)mm.

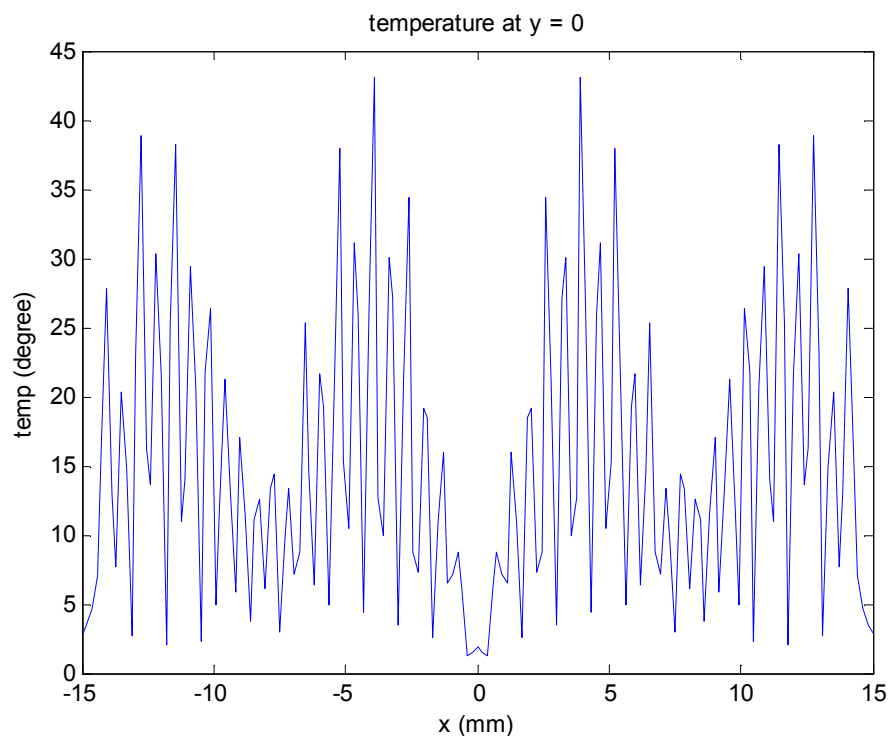


Figure 5. The temperature distribution in the treatment volume.

In thermal therapy simulations, the power deposition is generally modeled by Equation (3). The resulting power deposition provides the input to the BHTE, [15], which simulates the temperature distribution. To show the influence of waveform diversity method, simulation parameters on the calculated temperature, the bio-heat transfer model in Equation (4) is evaluated for the 10 rings array which generates a multiple focus at 38 mm tumor volume. In these simulations, the temperature field is computed in a 38 mm volume, where the boundaries of the computational grid are maintained at 37°C, the blood perfusion is 8 kg/m³/s, the thermal conductivity is 0.55 W/m/°C, and the specific heat of blood is 4000 J/kg/°C. The goal of each simulation is to elevate the temperature at the focus to be close to 45°C (therapeutic temperature) [15]. The temperature fields are shown in figure 5.

5. Conclusions

The pressure and temperature distributions are obtained by the waveform diversity method. The simulation results show that the peak tumor temperatures produced by spot scanning occur in the region of the tumor that is proximal to the phased array, and significant intervening tissue heating is also generated. Thus, waveform diversity combined with mode scanning generates multiple focus patterns that maximize the power delivered to the tumor when minimizing the power in other specified locations, and this combination improves the temperature localization relative to single focus spot scanning. The 10 concentric rings phased array discussed in this paper is used successfully to produce pressure leads to temperature with therapeutic values efficient to treat tumors in bladder. Finally, the phased array can be considered as an efficient non-invasive method for tumor treatments without surgery.

References

- [1] Xiaozheng Zeng and Robert J. McGough "Optimal simulations of the angular spectrum approach" *J. Acoust. Soc. Am.* 125 (5), (May 2009).
- [2] Xiaozheng (Jenny) Zeng, Jian Li Robert J. McGough "A Waveform Diversity Method for Optimizing 3-D Power Depositions Generated by Ultrasound Phased Array" *IEEE TRANSACTIONS ON BIOMEDICAL ENGINEERING*, VOL. 57, NO. 1, JANUARY (2010).
- [3] D. Liu and R. C. Wagg, "Propagation and backpropagation for ultrasonic wavefront design," *IEEE Trans. Ultrason. Ferroelectr. Freq. Control* 44, 1–13 (1997).
- [4] B. Guo and J. Li, "Waveform diversity based ultrasound system for hyperthermia treatment of breast cancer," *IEEE Trans. Biomed. Eng.*, vol. 55, no. 2, pp. 822–826, Feb. (2008).
- [5] P. Stoica, J. Li, X. Zhu, and B. Guo, "Waveform synthesis for diversity based transmit beam pattern design," *IEEE Trans. Signal Process.*, vol. 56, no. 6, pp. 2593–2598, Jun. (2008).
- [6] J. F. Sturm, "Using SeDuMi 1.02, a MATLAB toolbox for optimization over symmetric cones," *Optim. Methods Softw.*, vol. 11/12, pp. 625–653, (1999).
- [7] K. C. Toh, M. J. Todd, and R. H. Tutuncu, "SDPT3—A MATLAB software package for semidefinite programming," *Optim. Methods Softw.*, vol. 11, pp. 545–581, (1999).
- [8] M. S. Ibbini and C. A. Cain, "A field conjugation method for direct synthesis of hyperthermia phased-array heating patterns," *IEEE Trans. Ultrason., Ferroelectr. Freq. Control*, vol. 36, no. 2, pp. 3–9, Nov. (1989).
- [9] R. J. McGough, "Rapid calculations of time-harmonic nearfield pressures produced by rectangular piston," *J. Acoust. Soc. Amer.*, vol. 115, no. 5, pp. 1934–1941, (2004).
- [10] N. H. Ismail, A. T. Ibrahim "Temperature distribution in the human brain during ultrasound hyperthermia" *Journal of electromagnetic waves and applicators*, vol. 16, no. 6 pp. 803–811, (2002).
- [11] Kraft M. Approach to the patient with respiratory disease. In: Goldman L, Schafer AI, eds. *Goldman's Cecil Medicine*.
- [12] Kupeli E, Karnac D, Mehta AC. Flexible bronchoscopy. In: Mason RJ, Broaddus VC, Martin TR, et al., eds. *Textbook of Respiratory Medicine*.
- [13] Reynolds HY. Respiratory structure and function: mechanisms and testing. In: Goldman L, Schafer AI, eds. *Goldman's Cecil Medicine*.
- [14] R. J. McGough, H. Wang, E. S. Ebbini, and C. A. Cain, "Mode scanning: Heating pattern synthesis with ultrasound phased arrays," *Int. J. Hyperthermia*, vol. 10, no. 3, pp. 433–442, (1994).
- [15] P. R. Stauffer, "Evolving technology for thermal therapy of cancer," *Int. J. Hyperthermia* 21, 731C744 (2005).